

FedIA: Towards Domain-Robust Aggregation in Federated Graph Learning

Zhanting Zhou¹, Kahou Tam², Yiding Feng¹, Ziqiang Zheng¹, Zeyu Ma¹ and Yang Yang¹

¹University of Electronic Science and Technology of China

²State Key Laboratory of Internet of Things for Smart City, University of Macau

Abstract

Federated Graph Learning (FGL) enables a central server to coordinate model training across distributed clients without local graph data being shared. However, FGL significantly suffers from cross-silo domain shifts, where each "silo" (domain) contains a limited number of clients with distinct graph topologies. These heterogeneities induce divergent optimization trajectories, ultimately leading to global model divergence. In this work, we reveal a severe architectural pathology termed *Structural Orthogonality*: the topology-dependent message passing mechanism forces gradients from different domains to target disjoint coordinates in the parameter space. Through a controlled comparison between backbones, we statistically prove that GNN updates are near-perpendicular across domains (with projection ratios $\rightarrow 0$). Consequently, naive averaging leads to *Consensus Collapse*, a phenomenon where sparse, informative structural signals from individual domains are diluted by the near-zero updates of others. This forces the global model into a "sub-optimal" state that fails to represent domain-specific structural patterns, resulting in poor generalization. To address this, we propose FedIA, a lightweight server-side framework designed to reconcile update conflicts without auxiliary communication. FedIA operates in two stages: (1) **Global Importance Masking (GIM)** identifies a shared parameter subspace to filter out domain-specific structural noise and prevent signal dilution; (2) **Confidence-Aware Momentum Weighting (CAM)** dynamically re-weights client contributions based on gradient reliability to amplify stable optimization signals. Extensive experiments on multi-domain benchmarks for both homogeneous and heterogeneous graphs show that FedIA consistently outperforms 9 baselines across 2 GNN backbones, achieving accuracy improvements of up to 9.82%. Notably, FedIA maintains superior resilience against SOTA gradient inversion attacks while incurring zero additional communication overhead. CODE: <https://github.com/itoritsu/FedIA>.

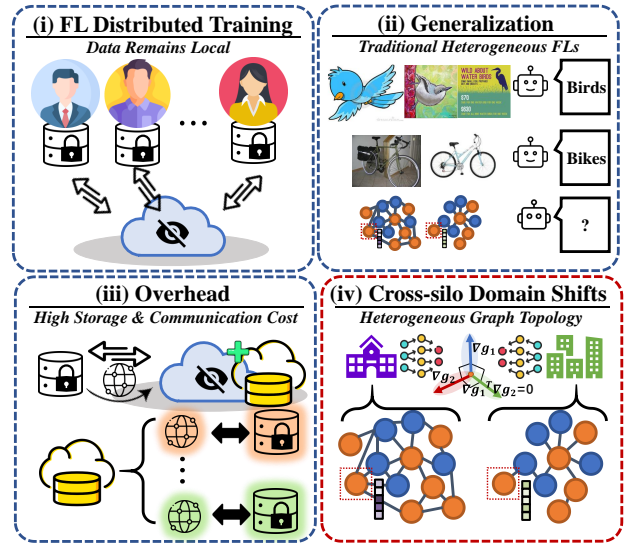


Figure 1: Challenges of FGL under domain shifts. (i) **FL distributed training:** clients collaborate without sharing raw data. (ii) **Generalization:** standard domain generalization targets unseen domains under distribution shift. (iii) **Overhead:** many approaches introduce non-trivial storage/communication costs. (iv) **Cross-silo domain shifts in FGL:** clients own different graph domains (sub-graphs) with heterogeneous topology and homophily; this alters message passing and can induce cross-domain update mismatch that existing domain-shift FGL methods do not fully resolve.

1 Introduction

Federated learning (FL) trains a shared model by having a central server orchestrate multiple clients to compute local updates while keeping raw data decentralized [McMahan *et al.*, 2017; Kairouz and McMahan, 2021]. Federated graph learning (FGL) extends this paradigm to graph-structured data that are naturally distributed across organizations, as in finance, healthcare, and recommendation, where each party owns a local subgraph and cannot directly pool the full graph due to privacy or policy constraints [Fu *et al.*, 2022; Li *et al.*, 2024]. Unlike grid-structured (Euclidean) data, graphs are non-Euclidean and couple node features with topology; message passing makes the computation flow explicitly depend on local connectivity [Bronstein *et al.*, 2017; Kipf, 2016; Wu

et al., 2020]. As a result, even when clients run the same training pipeline, distinct subgraph structures can induce different propagation semantics and thus different optimization behaviors.

We focus on *cross-silo* FGL, where each silo corresponds to one graph domain and may contain only a few clients (e.g., 1–2 subgraphs), in contrast to the massive cross-device setting [Kairouz and McMahan, 2021]. In such deployments, heterogeneity manifests as *domain shifts*: silos exhibit distinct topology and feature statistics, and collaboration is further constrained by data isolation and limited synchronization budgets. Figure 1 summarizes three practical challenges: (i) *distributed training under isolated data*, (ii) *generalization gaps across domains*, and (iii) *system overheads* that become severe when methods require extra communication channels or persistent server-side states.

Recent work such as FedSPA shows that structural heterogeneity (e.g., inconsistent homophily) can bias message passing and cause update direction conflicts across clients [Tan *et al.*, 2025]. In this work, we reveal a more severe pathology termed **Structural Orthogonality**: due to the topology-dependent computation flow in GNNs, updates from diverse domains tend to occupy disjoint coordinates in the parameter space rather than merely pointing in conflicting directions. This creates **Consensus Collapse**: as the overlap of salient supports diminishes, naive averaging (e.g., FedAvg [McMahan *et al.*, 2017]) increasingly dilutes sparse but informative coordinates (washed out by majority near-zeros), yielding a global model that is simultaneously sub-optimal for all domains.

General FL optimizers such as FedProx [Li *et al.*, 2020], FedDyn [Acar *et al.*, 2021], and MOON [Li *et al.*, 2021] mitigate client drift via regularization or local representation alignment, but they are primarily designed for non-IID sampling and do not directly resolve graph-induced structural conflicts that persist across domains [Tan *et al.*, 2025]. Meanwhile, specialized FGL solutions improve alignment but often trade effectiveness for system cost: prototype-based methods introduce extra communication beyond standard updates, while server-side masking or bookkeeping methods require persistent per-client statistics on the server, creating bottlenecks as model size and deployment scale grow [Wan *et al.*, 2024; Chen *et al.*, 2024]. This leaves a practical gap: *can we obtain domain-robust aggregation in cross-silo FGL by reusing the standard FL protocol, without adding extra payloads or heavy server state?*

To address this, we propose **FedIA**, a lightweight server-side framework. Our approach is grounded in the observation that gradients carry graph-coupled signals, allowing the server to identify the structural focus of each client directly through gradient magnitudes [Drencheva *et al.*, 2025]. The first stage, **Global Importance Masking**, avoids blindly averaging all parameters. Instead, FedIA identifies coordinates that are consistently salient across clients and uses a global mask to focus the aggregation on this structural consensus, filtering out domain-specific noise. The second stage, **Confidence-Aware Momentum Weighting**, addresses the fact that updates from different clients vary in reliability. We employ a momentum-based mechanism to track the reliability

of updates over time, amplifying stable signals while dampening erratic ones. This ensures a smooth training trajectory even under severe domain shifts. Across multi-domain benchmarks and GNN backbones, FedIA improves robustness to domain shifts over 9 baselines, while maintaining efficiency and empirical resilience against SOTA graph gradient inversion attacks [Drencheva *et al.*, 2025].

Our contributions are summarized as follows:

- We identify Structural Orthogonality as a backbone-dependent failure mode in FGL. By comparing GNNs with MLPs, we demonstrate that message passing forces updates into disjoint parameter coordinates. We formalize how this leads to Consensus Collapse, where naive averaging acts as a noise-injector by washing out salient local signals with majority near-zeros.
- We reveal that a two-stage server-side calibration effectively reconciles these geometric conflicts by first isolating a consistent structural consensus via **Global Importance Masking (GIM)** to prevent signal dilution, and then stabilizing aggregation through **Confidence-Aware Momentum Weighting (CAM)**. This design principle enables the server to recover domain-invariant features purely from standard updates without requiring auxiliary communication payloads.
- We verify the efficacy of FedIA across two GNN backbones and nine baselines on multi-domain benchmarks, achieving accuracy improvements of up to 9.82%. Our evaluation demonstrates that FedIA maintains superior efficiency with an $O(D)$ server memory footprint and zero additional communication overhead, while empirical stress-tests verify that the mechanism does not exacerbate reconstruction risks under SOTA gradient inversion attacks.

2 Related Works

Structural Heterogeneity and General FL Optimizers. FGL faces unique challenges where heterogeneity is not merely statistical but structural. Recent studies like FedSPA demonstrate that inconsistent topologies (e.g., homophily) induce divergent optimization trajectories, leading to “unpromising collaboration” [Tan *et al.*, 2025]. While general heterogeneity-aware FL optimizers (e.g., FedProx [Li *et al.*, 2020], FedDyn [Acar *et al.*, 2021], MOON [Li *et al.*, 2021]) mitigate drift via generic regularization, they often overlook these graph-specific structural mismatches. This creates a portability gap, calling for calibration mechanisms that explicitly reconcile conflicting update semantics rather than relying solely on generic client-side constraints.

Trade-offs in Existing FGL Solutions. Existing FGL methods improve cross-domain alignment but often introduce non-trivial system overheads. Prototype-based approaches (e.g., FGPP, FedPG) exchange auxiliary prototype vectors to align representations [Wan *et al.*, 2024; Wu *et al.*, 2025], which creates an extra synchronization channel and increases per-round communication beyond the standard update payload. Alternatively, server-side calibration methods (e.g., FedHEAL) mitigate conflicts via parameter selection and his-

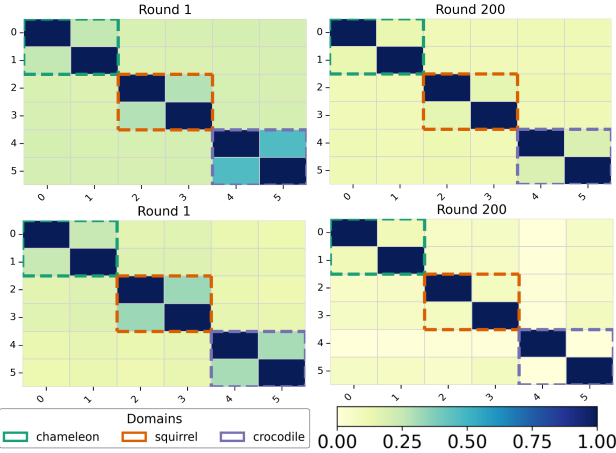


Figure 2: Pairwise Gradient Support Intersection (GSI; Jaccard overlap of top- $p\%$ coordinates) across clients. Early rounds show block-diagonal overlap, while late rounds approach near-identity under both FedAvg and FGFP, indicating *consensus collapse* in shared update supports.

torical bookkeeping [Chen *et al.*, 2024], but require maintaining client-specific statistics on the server, potentially scaling poorly with the number of clients. We also note two adjacent lines: (i) Byzantine-resilient robust aggregation with sparsification (e.g., LASA), which sparsifies updates and performs adaptive filtering to withstand malicious clients [Xu *et al.*, 2025b]; and (ii) system-/task-specific graph FL protocols (e.g., ENTENTE for cross-silo intrusion detection), which rely on reference graph synthesis and adaptive contribution scaling [Xu *et al.*, 2025a]. These methods target different objectives from benign domain shift, motivating a lightweight, protocol-preserving aggregation rule for practical domain-skewed FGL.

Positioning of FedIA. In contrast to prototype-based methods that demand auxiliary communication channels, and masking methods that require heavy persistent states, FedIA targets a lightweight server-side calibration. It operates purely on standard transmitted updates to reconcile structurally misaligned gradients, ensuring robustness without introducing extra payloads or memory bottlenecks.

3 Methodology

To address challenges from existing works as Section 2 shown, we propose the server-side domain-robust federated graph learning algorithm FedIA. In this section, we explain why we choose gradient as the FGL importance indicate in Section 3.1 and give a analysis for empirical motivation in Section 3.2. Section 3.3 introduce our FedIA with two stage framework.

3.1 Why Gradients? A Topology-Aware Update View

We consider node classification in domain-skewed Federated Graph Learning (FGL), where each client owns a graph domain with different feature statistics *and* different graph structures. Compared with standard FL, FGL introduces

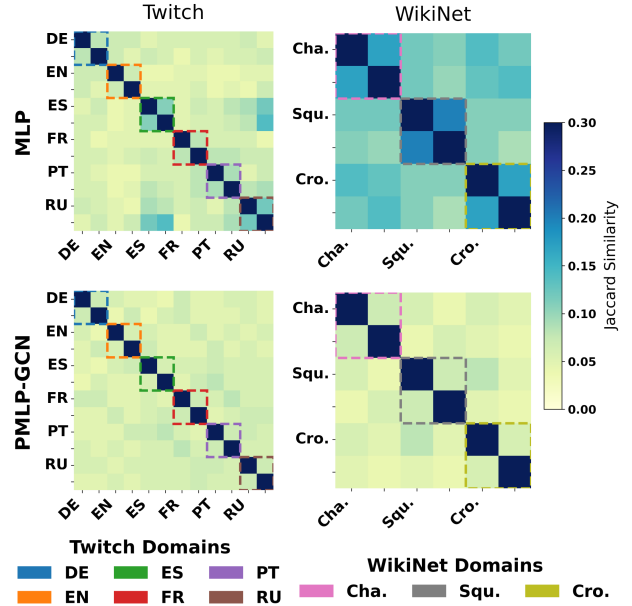


Figure 3: Backbone comparison of cross-domain update alignment. MLP retains higher inter-domain similarity, whereas PMLP-GCN shows weaker off-diagonal alignment across Twitch and WikiNet, suggesting message passing amplifies *structural orthogonality*.

an extra source of heterogeneity: the local topology (e.g., homophily) changes message passing behaviors, which can make clients learn with different inductive biases even under the same training pipeline. FedSPA explicitly formulates this as *homophily heterogeneity* and shows it can lead to homophily conflict and homophily bias, degrading collaboration in FGL [Tan *et al.*, 2025].

A unified object: local updates. In federated optimization, clients communicate either gradients or model deltas (e.g., FedAvg) [McMahan *et al.*, 2017]. We unify both as an update vector $u_k^{(t)}$ for client k at round t :

$$u_k^{(t)} \triangleq \begin{cases} g_k^{(t)} & (\text{gradient upload}), \\ -\frac{1}{\eta} \Delta W_k^{(t)} & (\text{model delta upload}). \end{cases} \quad (1)$$

This choice is practical and standard: under heterogeneity, local objectives differ and local training may deviate from the global descent direction (often described as *client drift*) [Karimireddy *et al.*, 2020].

Why updates are topology-dependent in GNNs. For message-passing GNNs, the computation graph is defined by the local adjacency, so the gradient depends on local topology:

$$g_k^{(t)} = \nabla_W \mathcal{L}_k = \sum_{v \in \mathcal{V}_k} \frac{\partial \mathcal{L}_k}{\partial h_v} \cdot \frac{\partial h_v}{\partial W}. \quad (2)$$

The term $\frac{\partial h_v}{\partial W}$ aggregates information from neighbors, which differs across clients when topologies differ. This topology dependence is supported by two independent threads: (i) GNN gradient inversion studies show that shared gradients can leak information about node features and even graph structure [Sinha *et al.*, 2024; Drencheva *et al.*,

2025]; (ii) gradient-flow interpretations view message passing as dynamics constrained by the underlying graph structure [Di Giovanni *et al.*, 2022].

Implication for robustness under domain shifts. Many recent FGL methods under domain shift focus on aligning representations using auxiliary objects (e.g., prototypes or structure proxies) [Wan *et al.*, 2024; Fu *et al.*, 2024]. These approaches improve semantic alignment, but they do not explicitly check whether clients still share (a) overlapping *salient update coordinates* or (b) consistent *update directions* over training. We therefore analyze $u_k^{(t)}$ directly and use the resulting observations to motivate our server-side aggregation design.

3.2 Observations and Motivations

Federated optimization under heterogeneity is known to suffer from objective inconsistency and client drift, which makes simple averaging unstable [McMahan *et al.*, 2017; Li *et al.*, 2020; Karimireddy *et al.*, 2020; Acar *et al.*, 2021; Kairouz and McMahan, 2021]. In domain-skewed FGL, topology differences further affect *which parameters get large updates* and *whether update directions agree across domains*. We make these two aspects explicit with simple measurements.

(A) Overlap of salient update coordinates. Let $g_t^{(k)}$ denote the gradient of client k at round t . We define the support set $S_t^{(k)}$ as the indices of the top- $p\%$ coordinates in $|g_t^{(k)}|$. For any pair (i, j) , Gradient Support Intersection (GSI) is:

$$\text{GSI}_t(i, j) = \frac{|S_t^{(i)} \cap S_t^{(j)}|}{|S_t^{(i)} \cup S_t^{(j)}|}. \quad (3)$$

Shrinking shared supports over training. Figure 2 shows that early rounds exhibit higher within-domain overlap (block-diagonal patterns), while later rounds approach a near-identity matrix under both FedAvg and FGGP. This indicates that clients progressively rely on increasingly different salient coordinates, i.e., the shared update supports collapse. A plausible interpretation is that different domains may end up optimizing different sparse effective subnetworks, consistent with the sparse-subnetwork perspective [Frankle and Carbin, 2018].

(B) Agreement of update directions and backbone effects. Support overlap alone does not tell whether remaining signals are aligned. We therefore examine cross-domain alignment under different backbones. Figures 3 & 4 compare MLP [Rosenblatt, 1957] and message-passing backbones (PMLP-GCN Yang *et al.* [2022]). The message-passing backbone shows weaker inter-domain alignment and a projection-ratio distribution concentrated near zero, suggesting near-orthogonal cross-domain updates. This backbone gap is consistent with the fact that message passing makes updates depend on topology (Section 3.1).

Motivation for aggregation. Together, these observations point to a concrete failure mode under domain shifts in FGL: (i) the set of salient update coordinates stops being shared across domains; and (ii) cross-domain update directions become weakly aligned, especially with message passing. Therefore, a practical server-side aggregator should (1)

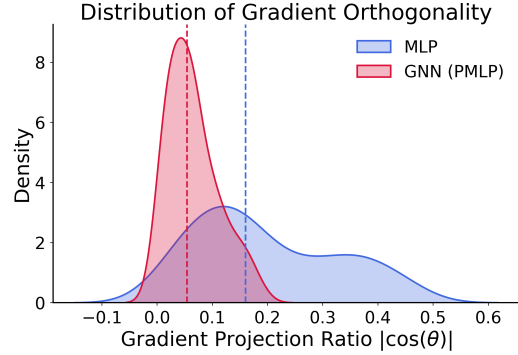


Figure 4: Distribution of gradient projection ratios ($|\cos \theta|$) across domains. Message-passing backbone concentrates near zero, indicating near-orthogonal updates, which motivates importance-aware aggregation to avoid cancellation in naive averaging.

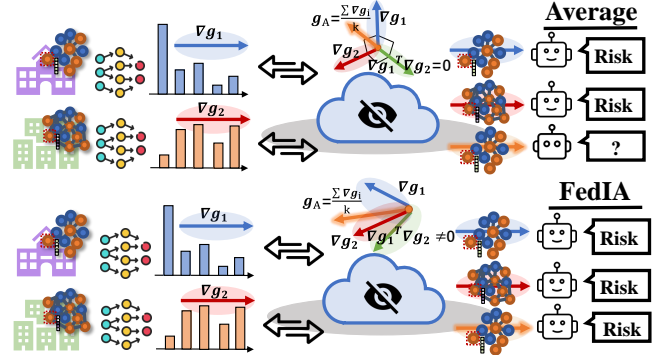


Figure 5: The aggregation workflow comparison between Average (FedAvg) and FedIA. Leveraging lightweight server-side interventions, FedIA alleviates the consensus collapse stemming from gradient orthogonality, which leads to a substantial improvement in global model performance.

preserve a small but globally consistent set of important coordinates, and (2) stabilize aggregation when client updates have uneven reliability. This directly motivates the two-stage design of FedIA.

3.3 Importance-Aware Aggregation

As shown in Figure 5, FedIA leverages lightweight server-side interventions to realize superior performance, makes aggregated global model more effective than Average. Specifically, FedIA targets the two empirical issues identified in Figure 2-4: (i) shared supports shrink over rounds (consensus collapse), and (ii) update confidence becomes uneven across domains (directional conflicts with varying strength). Accordingly, FedIA applies a two-stage, server-side gradient pre-conditioning pipeline as illustrated in Figure 6: **Stage-1** extracts a global shared subspace to reduce gradient dilution; **Stage-2** stabilizes aggregation within that subspace under uneven confidence.

Stage 1: Global Importance Masking (GIM)

Motivated by the shrinking overlap observed in Figure 2, naive averaging can wash out coordinates that are salient only to a subset of clients, i.e., dilution by majority near-zeros.

To preserve globally shared signals, the server builds a consensus subspace from the magnitude profile of participating clients.

At round t , each client $k \in \mathcal{S}_t$ uploads its gradient g_k^t . The server computes an importance vector

$$\tilde{g}^t = \frac{1}{|\mathcal{S}_t|} \sum_{k \in \mathcal{S}_t} |g_k^t|, \quad (4)$$

and keeps the top- ρ fraction of coordinates:

$$M^t = \text{TopRatioMask}(\tilde{g}^t, \rho) \in \{0, 1\}^d. \quad (5)$$

Each client gradient is then projected onto the shared subspace:

$$\hat{g}_k^t = g_k^t \odot M^t. \quad (6)$$

Relation to sparsified optimization. Top- k sparsification is often used for communication reduction and typically relies on memory/error-feedback for convergence [Lin *et al.*, 2017; Stich *et al.*, 2018]. FedIA uses the same top-coordinate principle without changing communication: the mask explicitly defines a shared subspace so that sparse but globally consistent coordinates are not diluted.

Stage 2: Confidence-Aware Momentum Weighting (CAM)

Stage-1 specifies *where* to aggregate; Stage-2 specifies *how much* to trust each client within the shared subspace. Under heterogeneity, clients can contribute updates of very different strength, yielding biased or unstable aggregation (objective inconsistency) [Wang *et al.*, 2021]. We therefore assign each client a confidence score using its masked-gradient energy:

$$s_k^t = \|\hat{g}_k^t\|_2, \quad (7)$$

convert scores to normalized weights, and apply an EMA to reduce round-wise noise from sampling and local stochasticity:

$$\alpha_k^t \leftarrow \beta \alpha_k^{t-1} + (1 - \beta) \cdot \frac{\exp(s_k^t)}{\sum_{j \in \mathcal{S}_t} \exp(s_j^t)}. \quad (8)$$

The global update is

$$g^t = \sum_{k \in \mathcal{S}_t} \alpha_k^t \hat{g}_k^t, \quad w^{t+1} = w^t - \eta g^t. \quad (9)$$

Why EMA on weights? Server-side momentum/adaptive updates are known to stabilize non-IID training [Hsu *et al.*, 2019; Reddi *et al.*, 2020a]. FedIA applies the same stabilization idea to contribution weights rather than model parameters: EMA smooths volatile per-round confidence while preserving Stage-1 subspace purification. Empirically, the improved cross-client color consistency shown in the right panel of Figure 6 indicates reduced domain-heterogeneity impact under FedIA. Algorithm 1 summarises the complete FedIA aggregation.

4 Experiments

In this section, we present extensive experiments and analyze the superior performances of FedIA. In Section 4.1, we introduce the basic information of these experiments. We show the performance comparison in the Section 4.2-4.4. Due to space limits, details please refer to Appendix A.

Algorithm 1 Federated Importance-Aware Aggregation

- 1: **Input:** Initial model W^0 , learning rate η , clients \mathcal{C} , \mathcal{S}_t is the selection subset of clients from \mathcal{C} , subspace ratio ρ .
- 2: **Server executes:**
- 3: Initialize client weights $\alpha_k^0 \leftarrow 1/|\mathcal{C}|$ for $k \in \mathcal{C}$.
- 4: **for** each round $t = 0, 1, \dots, T - 1$ **do**
- 5: $g^{t+1} \leftarrow \mathbf{0}$.
- 6: \triangleright **Stage 1:**
- 7: $\tilde{g}^{t+1} \leftarrow \frac{1}{|\mathcal{S}_t|} \sum_{k \in \mathcal{S}_t} |g_k^{t+1}|$.
- 8: $M^{t+1} \leftarrow \text{TopRatioMask}(\tilde{g}^{t+1}, \rho)$.
- 9: \triangleright **Stage 2:**
- 10: Calculate contribution score: $s_k^{t+1} \leftarrow \|g_k^{t+1} \odot M^{t+1}\|_2$
- 11: Update momentum weights:

$$\alpha_k^{t+1} \leftarrow \beta \alpha_k^t + (1 - \beta) \cdot \frac{\exp(s_k^{t+1})}{\sum_{j \in \mathcal{S}_t} \exp(s_j^{t+1})}$$
- 12: Aggregate: $g^{t+1} \leftarrow \sum_{k \in \mathcal{S}_t} \alpha_k^{t+1} (g_k^{t+1} \odot M^{t+1})$
- 13: $W^{t+1} \leftarrow W^t - \eta \cdot g^{t+1}$.
- 14: **end for**
- 15: **return** W^T .

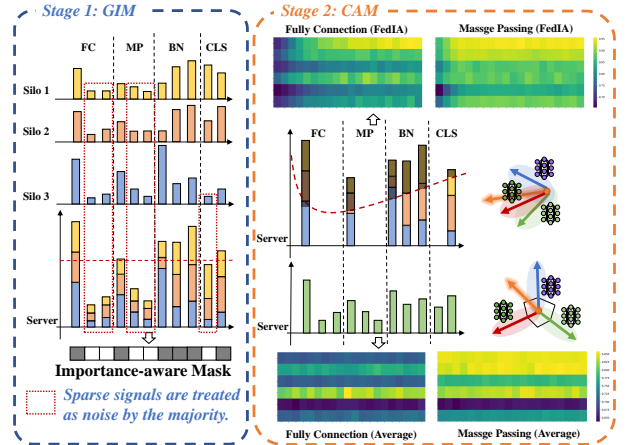


Figure 6: Two-stage design of FedIA. It presents FedIA addresses these issues via a two-stage aggregation mechanism: (1) global importance-aware masking and (2) module-wise confidence reweighting. This approach fosters consistent activation patterns (evidenced by more uniform heatmaps), demonstrating effective mitigation of domain shifts.

4.1 Setup

In our experiments, we configured the number of local iterations to 5. The local optimizer used is SGD [Robbins and Monro, 1951] with a momentum of 0.9 and a weight decay of $1e-5$. The local learning rate η is set at 0.01, and the communication rounds are set to 200. The hyperparameters of the FedIA framework include the mask ratio ρ and the momentum factor β . We defined the parameter search space for these hyperparameters as $\{0.1, 0.3, 0.5, 0.7, 0.9\}$. We conducted extensive experiments using 9 FL heterogeneity algorithms (introduced in Section 2) on two different graph neural network backbones and two kinds of multi-domain graph datasets. Detailed setups, including datasets, backbones and

Table 1: Accuracy comparison on the **Twitch Gamers** domain skew setting (Ratio 1:10:1:1:1:1, 30 Clients). Results are reported as mean($\%$) \pm std over the last 20 rounds. Methods are grouped pairwise (baseline vs. enhanced) with alternating gray shading. The column Δ denotes the accuracy gap relative to generic FedAvg. The colored superscripts (e.g., $\uparrow\Delta$ or $\downarrow\Delta$) indicate the specific performance gain/loss achieved by FedIA compared to the **original baseline** in that group. Notably, " \rightarrow FedIA" in the FedSPA group represents an ablation where FedSPA's native HBDA aggregator is replaced by FedIA.

Methods	Domains						Overall	
	ES	DE	FR	RU	EN	PT	AVG	Δ
FedAvg ^{baseline} to Δ	66.98 \pm 0.06	38.76 \pm 0.01	59.38 \pm 0.05	65.06 \pm 0.02	48.87 \pm 0.03	59.97 \pm 0.10	56.50 \pm 0.04	-
+ FedIA	71.29 \pm 0.00	38.95 \pm 0.00	62.75 \pm 0.00	76.40 \pm 0.00	45.53 \pm 0.00	64.02 \pm 0.00	59.82 \pm 0.00	+3.32 ^{\uparrow3.32}
FedProx	66.45 \pm 0.00	38.47 \pm 0.00	59.63 \pm 0.00	65.55 \pm 0.03	48.02 \pm 0.01	59.48 \pm 0.00	56.27 \pm 0.01	-0.23
+ FedIA	69.98 \pm 0.18	50.57 \pm 0.15	62.56 \pm 0.17	73.29 \pm 0.16	55.37 \pm 0.47	68.85 \pm 0.37	63.44 \pm 0.11	+6.94 ^{\uparrow7.17}
MOON	66.95 \pm 0.02	38.76 \pm 0.01	59.56 \pm 0.00	65.52 \pm 0.02	48.58 \pm 0.03	59.74 \pm 0.00	56.52 \pm 0.01	+0.02
+ FedIA	69.95 \pm 0.06	43.33 \pm 0.03	62.42 \pm 0.07	71.56 \pm 0.04	51.49 \pm 0.04	63.58 \pm 0.05	60.39 \pm 0.03	+3.89 ^{\uparrow3.87}
FedDyn	50.00 \pm 21.29	50.00 \pm 11.05	50.00 \pm 14.02	50.03 \pm 26.37	50.00 \pm 4.47	50.00 \pm 12.75	50.01 \pm 9.81	-6.50
+ FedIA	71.29 \pm 0.00	38.95 \pm 0.00	62.75 \pm 0.00	76.40 \pm 0.00	45.50 \pm 0.01	64.02 \pm 0.00	59.82 \pm 0.00	+3.32 ^{\uparrow9.82}
FedProto	67.11 \pm 0.09	38.78 \pm 0.01	59.49 \pm 0.06	65.15 \pm 0.03	48.92 \pm 0.02	59.87 \pm 0.00	56.55 \pm 0.02	+0.05
+ FedIA	62.42 \pm 0.06	54.40 \pm 0.05	60.48 \pm 0.02	63.50 \pm 0.20	56.99 \pm 0.06	61.30 \pm 0.04	59.85 \pm 0.05	+3.35 ^{\uparrow3.30}
FGSSL	67.19 \pm 0.12	38.97 \pm 0.02	59.58 \pm 0.04	65.36 \pm 0.04	50.01 \pm 0.04	59.35 \pm 0.00	56.74 \pm 0.02	+0.24
+ FedIA	68.40 \pm 0.03	51.72 \pm 0.03	60.46 \pm 0.02	69.10 \pm 0.02	54.03 \pm 0.03	63.39 \pm 0.04	61.18 \pm 0.01	+4.68 ^{\uparrow3.75}
FGGP	63.51 \pm 10.49	65.73 \pm 1.09	54.71 \pm 6.60	61.21 \pm 13.15	55.67 \pm 2.30	63.36 \pm 8.55	60.70 \pm 6.03	+4.20
+ FedIA	72.05 \pm 1.28	51.84 \pm 1.74	63.17 \pm 1.85	73.18 \pm 2.17	58.45 \pm 2.11	68.01 \pm 0.57	64.45 \pm 0.38	+7.95 ^{\uparrow4.44}
FedSPA	61.37 \pm 0.02	51.81 \pm 0.02	52.77 \pm 0.02	63.30 \pm 0.03	60.60 \pm 0.04	58.80 \pm 0.02	58.13 \pm 0.04	+1.63
\rightarrow FedIA	61.88 \pm 0.03	51.86 \pm 0.02	58.69 \pm 0.01	62.60 \pm 0.04	56.24 \pm 0.02	59.50 \pm 0.03	58.45 \pm 0.04	+1.95 ^{\uparrow0.32}
+ FedIA	65.29 \pm 0.23	50.95 \pm 0.02	61.02 \pm 0.10	70.40 \pm 0.24	51.53 \pm 0.09	62.75 \pm 0.04	59.80 \pm 0.14	+3.30 ^{\uparrow1.73}

Table 2: Accuracy on **WikiNet** cross-domain setting (Ratio 1:1:1, 6 Clients). Other annotations and settings are the same to Table 1. Cha. means Domain Chameleon, Cro. means Domain Crocodile, and Squ. means Domain Squirrel.

Methods	Domains			Overall	
	Cha.	Cro.	Squ.	AVG	Δ
FedAvg ^{baseline} to Δ	12.77	7.15	12.45	10.79	-
+ FedIA	25.02	20.55	21.54	15.10	+4.31 ^{\uparrow4.31}
FedProx	12.06	5.72	10.14	9.31	-1.48
+ FedIA	14.31	4.21	13.44	10.65	+0.14 ^{\uparrow1.34}
MOON	12.72	6.83	12.56	10.70	-0.09
+ FedIA	16.54	10.13	14.28	13.65	+2.86 ^{\uparrow2.95}
FedDyn	15.45	8.50	13.46	12.47	+1.68
+ FedIA	20.41	14.22	19.33	17.98	+7.19 ^{\uparrow5.51}
FedProc	10.55	12.61	6.75	12.29	+1.50
+ FedIA	20.04	10.34	19.96	16.78	+5.99 ^{\uparrow4.46}
FedProto	12.65	7.16	12.48	10.76	-0.03
+ FedIA	21.46	15.07	21.25	19.26	+8.47 ^{\uparrow8.50}
FGSSL	14.45	7.97	13.64	12.02	+1.23
+ FedIA	14.50	7.92	13.74	12.12	+1.43 ^{\uparrow0.20}
FGGP	29.25	42.79	14.78	28.94	+18.15
+ FedIA	42.99	14.86	29.21	29.02	+18.23 ^{\uparrow0.08}
FedSPA	37.46	23.34	38.51	33.10	+22.31
\rightarrow FedIA	37.34	23.18	38.51	33.01	+22.22 ^{\downarrow0.09}
+ FedIA	37.44	23.49	38.57	33.17	+22.38 ^{\uparrow0.07}

baselines, are shown in Appendix A.

4.2 Performance Comparison Across Domains

We evaluate the robustness of FedIA on Twitch Gamers and WikiNet benchmarks as reported in Table 1 and Table 2. The

results demonstrate that FedIA consistently enhances performance across diverse federated optimizers such as FedProx and FedDyn. Notably, FedDyn suffers from severe strategy degradation under significant domain shifts with accuracy dropping to 50.00% in Table 1. FedIA successfully restores its functionality by filtering invalid gradient information effectively. While FGGP generally outperforms FedSPA under identical settings, it exhibits high variance in Table 1. Figure 7 further reveals that FGGP suffers from severe convergence oscillation regardless of hyperparameter adjustments. In contrast, FedIA guarantees stability even at a high learning rate of 0.01. This implies that FGGP relies heavily on prototypes while overlooking the intrinsic relationship between domain heterogeneity and gradient conflicts which FedIA explicitly addresses.

4.3 Performance Comparison Across Backbones

We extend our evaluation to the GraphSage backbone using FedSage as a representative baseline in Table 3. The results indicate that FedIA consistently improves the average domain accuracy for both the generic FedAvg and the specialized FedSage framework. This confirms that the challenges of structural heterogeneity persist across different model architectures. Our method effectively mitigates these issues and demonstrates strong compatibility beyond specific GNN designs.

4.4 Performance Comparison of Aggregation

Figure 8 compares aggregation rules under two federation pipelines (FedAvg and FGGP) and two shift regimes (cross-domain and domain skew). FedIA consistently achieves the best performance across all settings. Importantly, FedIA re-

Table 3: Comparison with FedSage on **GraphSage** backbone. The pairwise grouping highlights the improvement FedIA brings to both generic and specialized pipelines. Other annotations and settings are the same to Table 1.

Methods	Domains						Overall	
	ES	DE	FR	RU	EN	PT	AVG	Δ
FedAvg ^{baseline} _{to Δ}	31.29 \pm 0.25	61.05 \pm 0.06	37.31 \pm 0.48	25.39 \pm 0.35	54.05 \pm 0.16	38.08 \pm 0.25	41.19 \pm 0.20	—
+ FedIA	39.38 \pm 0.51	43.18 \pm 0.30	37.98 \pm 0.18	46.07 \pm 0.64	51.67 \pm 0.07	47.52 \pm 0.83	44.30 \pm 0.27	+3.11 ^{↑3.11}
FedSage	70.70 \pm 0.00	38.95 \pm 0.00	63.23 \pm 0.03	75.66 \pm 0.00	44.79 \pm 0.02	62.75 \pm 0.00	59.35 \pm 0.01	+18.16
+ FedIA	71.30 \pm 0.02	38.95 \pm 0.01	64.02 \pm 0.00	76.39 \pm 0.03	45.53 \pm 0.01	62.75 \pm 0.00	59.82 \pm 0.01	+18.73 ^{↑0.57}

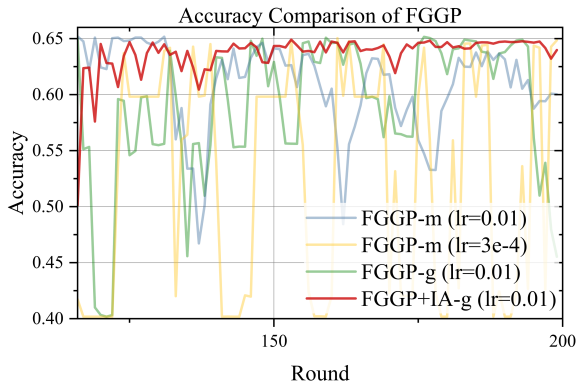


Figure 7: FedIA mitigates the convergence volatility observed in SOTA methods like FGPP. FedIA improves accuracy and stabilizes convergence of FGPP under both model-parameter-communication (-m; original setting in [Wan *et al.*, 2024]) and gradient-communication (-g) upload settings.

mains compatible with advanced FGL pipelines: while some server-side calibration baselines may improve FedAvg yet degrade FGPP, FedIA yields robust gains in both pipelines. We additionally report LASA [Xu *et al.*, 2025b] and ENTENTE [Xu *et al.*, 2025a] as representative robust/system-specific baselines. Both can underperform the vanilla baseline in our *benign* domain-shift setting, suggesting that objectives optimized for Byzantine resilience (LASA) or intrusion-detection-oriented graph protocols (ENTENTE) may trade utility for conservatism when client heterogeneity is non-adversarial.

Beyond accuracy, FedIA is designed for practical deployments with strict system budgets. FedHEAL-style book-keeping requires maintaining client-specific historical statistics/masks on the server, which scales as $\mathcal{O}(N \times D)$ for N clients and D model parameters, creating a memory bottleneck as N grows. In contrast, FedIA operates on the aggregated global update and maintains only a single global mask buffer, reducing server memory to $\mathcal{O}(D)$ (independent of N). Moreover, prototype-based FGL methods introduce an auxiliary communication channel for prototype exchange, adding $\mathcal{O}(P)$ payload per round for prototype size P , while FedIA stays within the standard update transmission protocol and does not require extra synchronization channels.

4.5 The concern of Gradient Inversion

Gradient inversion is a known risk in gradient-sharing systems (e.g., DLG [Zhu *et al.*, 2019]) and has recently been

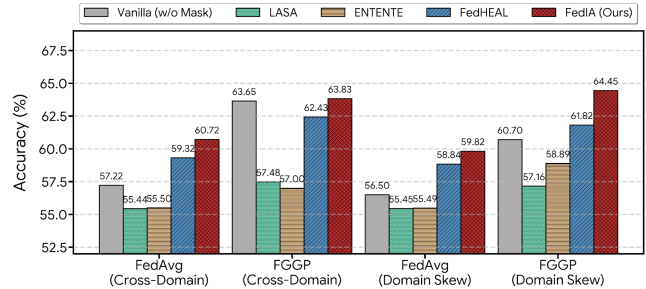


Figure 8: Performance comparison of aggregation strategies under domain shifts on FedAvg and FGPP. We evaluate five server-side aggregation: vanilla aggregation (w/o mask), LASA [Xu *et al.*, 2025b], ENTENTE [Xu *et al.*, 2025a], FedHEAL [Chen *et al.*, 2024], and FedIA (ours).

strengthened for graph data by GRAIN [Drencheva *et al.*, 2025]. Here we ask a narrower question: whether our server-side calibration in FedIA *increases* inversion risk compared to the same pipeline without FedIA.

We stress-test FedIA using GRAIN and report inversion-related metrics on 62 different runs. FedIA reduces the privacy score by 4.0% (0.519 \rightarrow 0.498). This result provides risk-oriented evidence that FedIA **does not exacerbate** gradient inversion under our evaluated settings.

5 Conclusion

In this work, we addressed the critical challenge of structural domain shifts in FGL. Through a comprehensive empirical analysis, we identified **Structural Orthogonality** as a primary failure mode: due to the topology-dependent message-passing mechanism, updates from different domains target disjoint coordinates in the parameter space. This phenomenon leads to *Consensus Collapse*, where naive averaging dilutes salient structural signals into background noise.

To resolve these issues, we proposed *FedIA*, a lightweight server-side framework that reconciles update conflicts without auxiliary communication or persistent state. FedIA operationalizes a two-stage calibration: (1) **Global Importance Masking** to isolate the structural consensus and filter out domain-specific noise, and (2) **Confidence-Aware Momentum Weighting** to stabilize aggregation under uneven update strengths. Extensive experiments demonstrate that FedIA consistently outperforms 9 baselines across multiple GNN backbones, achieving accuracy improvements of up to **9.82%**.

References

- Durmus Alp Emre Acar, Yue Zhao, Ramon Matas Navarro, Matthew Mattina, Paul N Whatmough, and Venkatesh Saligrama. Federated learning based on dynamic regularization. *arXiv preprint arXiv:2111.04263*, 2021.
- Michael M Bronstein, Joan Bruna, Yann LeCun, Arthur Szlam, and Pierre Vandergheynst. Geometric deep learning: going beyond euclidean data. *IEEE Signal Processing Magazine*, 34(4):18–42, 2017.
- Yuhang Chen, Wenke Huang, and Mang Ye. Fair federated learning under domain skew with local consistency and domain diversity. In *Proceedings of the IEEE/CVF Conference on Computer Vision and Pattern Recognition*, pages 12077–12086, 2024.
- Francesco Di Giovanni, James Rowbottom, Benjamin P Chamberlain, Thomas Markovich, and Michael M Bronstein. Graph neural networks as gradient flows: understanding graph convolutions via energy. *arXiv preprint arXiv:2206.10991*, 2022.
- Maria Drencheva, Ivo Petrov, Maximilian Baader, Dimitar I Dimitrov, and Martin Vechev. Grain: Exact graph reconstruction from gradients. *arXiv preprint arXiv:2503.01838*, 2025.
- Matthias Fey and Jan Eric Lenssen. Fast graph representation learning with pytorch geometric, 2019.
- Jonathan Frankle and Michael Carbin. The lottery ticket hypothesis: Finding sparse, trainable neural networks. *arXiv preprint arXiv:1803.03635*, 2018.
- Xingbo Fu, Binchi Zhang, Yushun Dong, Chen Chen, and Jundong Li. Federated graph machine learning: A survey of concepts, techniques, and applications. *ACM SIGKDD Explorations Newsletter*, 24(2):32–47, 2022.
- Xingbo Fu, Zihan Chen, Binchi Zhang, Chen Chen, and Jundong Li. Federated graph learning with structure proxy alignment. In *Proceedings of the 30th ACM SIGKDD Conference on Knowledge Discovery and Data Mining*, pages 827–838, 2024.
- Will Hamilton, Zhitao Ying, and Jure Leskovec. Inductive representation learning on large graphs. *Advances in neural information processing systems*, 30, 2017.
- Tzu-Ming Harry Hsu, Hang Qi, and Matthew Brown. Measuring the effects of non-identical data distribution for federated visual classification. *arXiv preprint arXiv:1909.06335*, 2019.
- Wenke Huang, Guancheng Wan, Mang Ye, and Bo Du. Federated graph semantic and structural learning. *arXiv preprint arXiv:2406.18937*, 2024.
- Peter Kairouz and H Brendan McMahan. Advances and open problems in federated learning. *Foundations and trends in machine learning*, 14(1-2):1–210, 2021.
- Sai Praneeth Karimireddy, Satyen Kale, Mehryar Mohri, Sashank Reddi, Sebastian Stich, and Ananda Theertha Suresh. Scaffold: Stochastic controlled averaging for federated learning. In *International conference on machine learning*, pages 5132–5143. PMLR, 2020.
- TN Kipf. Semi-supervised classification with graph convolutional networks. *arXiv preprint arXiv:1609.02907*, 2016.
- Tian Li, Anit Kumar Sahu, Manzil Zaheer, Maziar Sanjabi, Amreet Talwalkar, and Virginia Smith. Federated optimization in heterogeneous networks. *Proceedings of Machine Learning and Systems*, 2:429–450, 2020.
- Qinbin Li, Bingsheng He, and Dawn Song. Model-contrastive federated learning. In *Proceedings of the IEEE/CVF conference on computer vision and pattern recognition*, pages 10713–10722, 2021.
- Xunkai Li, Zhengyu Wu, Wentao Zhang, Yinlin Zhu, Ronghua Li, and Guoren Wang. Fedgta: Topology-aware averaging for federated graph learning. *arXiv preprint arXiv:2401.11755*, 2024.
- Yujun Lin, Song Han, Huizi Mao, Yu Wang, and William J Dally. Deep gradient compression: Reducing the communication bandwidth for distributed training. *arXiv preprint arXiv:1712.01887*, 2017.
- Brendan McMahan, Eider Moore, Daniel Ramage, Seth Hampson, and Blaise Aguera y Arcas. Communication-efficient learning of deep networks from decentralized data. In *Artificial intelligence and statistics*, pages 1273–1282. PMLR, 2017.
- Xutong Mu, Yulong Shen, Ke Cheng, Xueli Geng, Jiaxuan Fu, Tao Zhang, and Zhiwei Zhang. Fedproc: Prototypical contrastive federated learning on non-iid data. *Future Generation Computer Systems*, 143:93–104, 2023.
- Sashank Reddi, Zachary Charles, Manzil Zaheer, Zachary Garrett, Keith Rush, Jakub Konečný, Sanjiv Kumar, and H Brendan McMahan. Adaptive federated optimization. *arXiv preprint arXiv:2003.00295*, 2020.
- Sashank Reddi, Zachary Charles, Manzil Zaheer, Zachary Garrett, Keith Rush, Jakub Konečný, Sanjiv Kumar, and H Brendan McMahan. Adaptive federated optimization. *arXiv preprint arXiv:2003.00295*, 2020.
- Herbert Robbins and Sutton Monro. A stochastic approximation method. *The annals of mathematical statistics*, pages 400–407, 1951.
- Frank Rosenblatt. *The perceptron, a perceiving and recognizing automaton:(Project Para)*. Cornell Aeronautical Laboratory, 1957.
- Benedek Rozemberczki, Carl Allen, and Rik Sarkar. Multi-scale attributed node embedding. *Journal of Complex Networks*, 9(2):cnab014, 2021.
- Benedek Rozemberczki, Carl Allen, and Rik Sarkar. Multi-scale attributed node embedding. *Journal of Complex Networks*, 9(2):cnab014, 2021.
- Divya Anand Sinha, Ruijie Du, Yezi Liu, Athina Markopolou, and Yanning Shen. Gradient inversion attack on graph neural networks. *arXiv preprint arXiv:2411.19440*, 2024.
- Sebastian U Stich, Jean-Baptiste Cordonnier, and Martin Jaggi. Sparsified sgd with memory. *Advances in neural information processing systems*, 31, 2018.

- Yue Tan, Guodong Long, Lu Liu, Tianyi Zhou, Qinghua Lu, Jing Jiang, and Chengqi Zhang. Fedproto: Federated prototype learning across heterogeneous clients. In *Proceedings of the AAAI Conference on Artificial Intelligence*, volume 36, pages 8432–8440, 2022.
- Zihan Tan, Guancheng Wan, Wenke Huang, and Mang Ye. Fedssp: Federated graph learning with spectral knowledge and personalized preference. *arXiv preprint arXiv:2410.20105*, 2024.
- Zihan Tan, Guancheng Wan, Wenke Huang, He Li, Guibin Zhang, Carl Yang, and Mang Ye. Fedspa: Generalizable federated graph learning under homophily heterogeneity. In *Proceedings of the Computer Vision and Pattern Recognition Conference*, pages 15464–15475, 2025.
- Guancheng Wan, Wenke Huang, and Mang Ye. Federated graph learning under domain shift with generalizable prototypes. In *Proceedings of the AAAI Conference on Artificial Intelligence*, volume 38, pages 15429–15437, 2024.
- Jianyu Wang, Qinghua Liu, Hao Liang, Gauri Joshi, and H Vincent Poor. A novel framework for the analysis and design of heterogeneous federated learning. *IEEE Transactions on Signal Processing*, 69:5234–5249, 2021.
- Zonghan Wu, Shirui Pan, Fengwen Chen, Guodong Long, Chengqi Zhang, and Philip S Yu. A comprehensive survey on graph neural networks. *IEEE transactions on neural networks and learning systems*, 32(1):4–24, 2020.
- Zhengyu Wu, Xunkai Li, Yinlin Zhu, Rong-Hua Li, Guoren Wang, and Chenghu Zhou. Federated prototype graph learning. *arXiv preprint arXiv:2504.09493*, 2025.
- Jiacen Xu, Chenang Li, Yu Zheng, and Zhou Li. Entente: Cross-silo intrusion detection on network log graphs with federated learning. *arXiv preprint arXiv:2503.14284*, 2025.
- Jiahao Xu, Zikai Zhang, and Rui Hu. Achieving byzantine-resilient federated learning via layer-adaptive sparsified model aggregation. In *2025 IEEE/CVF Winter Conference on Applications of Computer Vision (WACV)*, pages 1508–1517. IEEE, 2025.
- Chenxiao Yang, Qitian Wu, Jiahua Wang, and Junchi Yan. Graph neural networks are inherently good generalizers: Insights by bridging gnns and mlps. *arXiv preprint arXiv:2212.09034*, 2022.
- Ligeng Zhu, Zhijian Liu, and Song Han. Deep leakage from gradients. *Advances in neural information processing systems*, 32, 2019.

A Detailed Experiments

In this appendix, we provide a detailed account of our experimental procedures and supplementary results to ensure full reproducibility and offer deeper insights into the performance of FedIA.

We begin by presenting the **Detailed Setup**, which outlines our computing environment, the rationale for dataset selection, data partitioning strategies for creating cross-domain and domain-skew scenarios, and comprehensive descriptions of all backbone models and baseline methods.

Following this, the **Detailed Performance Analysis** section offers an in-depth examination of FedIA’s performance on both the Twitch and WikiNet datasets, and includes a dedicated comparison on the GraphSage backbone to demonstrate FedIA’s generalizability.

Subsequently, we present an **Ablation Test** that deconstructs the FedIA framework to empirically validate the individual contributions of its core components.

Finally, we analyze the **Hyper-parameter Robustness**, investigating the sensitivity of FedIA and demonstrating its practical plug-and-play nature. Together, these sections provide a comprehensive empirical foundation for the claims made in the main paper.

A.1 Detailed Setup

We conducted experiments using NVIDIA GeForce RTX 4080 hardware, CUDA Driver 12.6, Driver Version 561.17, and Python 3.11 as our experimental environment. In our experiments, we configured the number of local iterations to 5. The local optimizer used is SGD [Robbins and Monro, 1951] with a momentum of 0.9 and a weight decay of $1e-5$. The local learning rate η is set at 0.01 for Twitch and 0.005 for WikiNet, and the communication rounds are set to 200. Following is more detailed setup.

Datasets

To achieve a fair and effective comparison in our study, we selected the dataset based on the following rationale: (1) To enhance the experimental reliability, we opted for datasets that are publicly available, sourced from the same interface, yet encompass different domains. (2) To minimize the effects of model heterogeneity, we chose datasets with consistent feature dimensions and label categories. (3) The dataset inherently exhibits cross-domain characteristics, enabling the development of domain skew experimental scenarios through random partitioning. Taking these factors into account, we chose the Twitch Gamers Dataset (e.g. **TwTich**) [Rozemberczki *et al.*, 2021a] and Wikipedia Network Dataset (e.g. **WikiNet**) [Rozemberczki *et al.*, 2021b] from the homogeneity collection of PyG library [Fey and Lenssen, 2019].

The **Twitch** Gamer networks dataset encompasses six domains: DE, EN, ES, FR, PT, and RU. Each domain features 128-dimensional node attributes, with all nodes representing binary classifications. Specifically, the DE domain comprises 9,498 nodes and 315,774 edges; the EN domain includes 7,126 nodes and 77,774 edges; the ES domain consists of 4,648 nodes and 123,412 edges; the FR domain contains 6,551 nodes and 231,883 edges; the PT domain features 1,912 nodes and 64,510 edges; and the RU domain has 4,385

nodes and 78,993 edges. Given that the DE domain has the highest number of nodes and edges, our design for addressing domain skew is primarily focused on this domain.

The **Wikipedia Networks** dataset collection includes three networks: chameleon, crocodile, and squirrel. In these networks, nodes represent Wikipedia articles, and edges indicate mutual links between them. Each network features multi-dimensional node attributes derived from bag-of-words representations of the articles, and all nodes are classified into one of five categories. Specifically, the chameleon network comprises 2,277 nodes and 36,101 edges, with 2,089-dimensional features. The crocodile network consists of 11,631 nodes and 170,918 edges, with 2,089-dimensional features. The squirrel network contains 5,201 nodes and 217,073 edges, also with 2,089-dimensional features. Given that the squirrel network has the highest number of edges, our design for addressing network density would be primarily focused on this network.

For the cross-domain experimental dataset, we directly utilized the same number of client with Twitch Gamers network (as setting 1 with 12 clients; and 6 clients for WikiNet). For the domain skew experimental dataset, we performed a random split of the DE domain, which contains the highest number of nodes within the Twitch Gamers network. This domain was subdivided into datasets with 5-fold (as setting 2 with 20 clients) and 10-fold (as setting 3 with 30 clients) allocations relative to the other domains, distributed among the clients. The graphs are partitioned into different subgraphs allocated to each client. To conduct the experiments uniformly and fairly, we split the nodes into train/valid/test sets, where the ratio is 60%:20%:20%. To mitigate the impact of statistical heterogeneity, our experiments employed a fully participatory setting.

Baselines & Backbone

We employed **PMLP-GCN**, utilize the 2 layers feature extractor and set the hidden layer size of 128, as the backbone for our major experiments [Yang *et al.*, 2022]; and employed **GraphSAGE**-mean [Hamilton *et al.*, 2017], utilizing a 2-layer neighborhood aggregation ($K = 2$, fan-outs of 25 and 10) and set the hidden embedding dimension to 128 as another backbone for our FedSage Comparison experiments. The baseline methods we utilized include: **FedAvg** [McMahan *et al.*, 2017] iteratively averages client model parameters to form a global model, serving as the classical baseline for communication-efficient federated optimization. **FedProx** [Li *et al.*, 2020] introduces a proximal term into each client’s objective to curb local drift, yielding stabler convergence under pronounced systems and statistical heterogeneity. **Moon** [Li *et al.*, 2021] leverages model-level contrastive learning between local and global representations to align feature spaces and counteract non-IID data effects. **FedDyn** [Acar *et al.*, 2021] adds a dynamic regularizer—effectively a control variate—that steers local optima toward the global objective, accelerating convergence without extra communication. **FedOPT** [Reddi *et al.*, 2020b] generalizes FedAvg by applying adaptive server-side optimizers (e.g., Adam, Yogi) to aggregated updates, improving learning speed and robustness on diverse clients. **FedProc** [Mu *et al.*, 2023] employs a prototypical contrastive loss that distills global class prototypes to

Table 4: Accuracy comparison on the **Twitch Gamers** cross-domain setting (Ratio 1:1:1:1:1, 12 Clients). Results are reported as mean \pm std over the last 20 rounds. Methods are grouped pairwise (baseline vs. enhanced) with alternating gray shading. **Annotations:** The column Δ denotes the accuracy gap relative to generic FedAvg. The colored superscripts (e.g., $\uparrow^{3.50}$) indicate the specific performance gain achieved by FedIA compared to the **original baseline** in that group.

Methods	Domains						Overall	
	ES	DE	FR	RU	EN	PT	AVG	Δ
FedAvg	66.46 \pm 0.02	38.38 \pm 0.02	58.84 \pm 0.03	68.74 \pm 0.03	49.36 \pm 0.02	61.57 \pm 0.00	57.22 \pm 0.01	-
+ FedIA	64.77 \pm 0.05	55.90 \pm 0.03	58.72 \pm 0.03	65.41 \pm 0.06	58.66 \pm 0.04	60.85 \pm 0.04	60.72 \pm 0.02	+3.50 $\uparrow^{3.50}$
FedProx	65.70 \pm 0.00	38.20 \pm 0.01	58.45 \pm 0.00	68.37 \pm 0.02	48.73 \pm 0.01	61.31 \pm 0.00	56.79 \pm 0.00	-0.43
+ FedIA	70.81 \pm 0.08	51.44 \pm 0.14	60.07 \pm 0.10	73.34 \pm 0.10	53.28 \pm 0.06	68.73 \pm 0.09	62.95 \pm 0.05	+5.73 $\uparrow^{6.16}$
MOON	66.55 \pm 0.02	38.37 \pm 0.00	58.70 \pm 0.02	68.95 \pm 0.06	49.18 \pm 0.02	61.46 \pm 0.05	57.20 \pm 0.01	-0.02
+ FedIA	70.48 \pm 0.00	38.95 \pm 0.00	62.23 \pm 0.00	76.57 \pm 0.00	46.05 \pm 0.00	66.41 \pm 0.00	60.11 \pm 0.00	+2.89 $\uparrow^{2.91}$
FedDyn	67.51 \pm 0.34	38.86 \pm 0.13	59.45 \pm 0.21	70.83 \pm 0.11	49.31 \pm 0.30	63.65 \pm 0.19	58.27 \pm 0.14	+1.05
+ FedIA	69.81 \pm 0.49	53.35 \pm 0.63	61.28 \pm 0.08	69.84 \pm 0.11	56.12 \pm 0.26	68.82 \pm 0.40	63.20 \pm 0.06	+5.98 $\uparrow^{4.93}$
FedProc	66.46 \pm 0.02	38.35 \pm 0.01	58.74 \pm 0.03	68.65 \pm 0.03	49.29 \pm 0.02	61.57 \pm 0.00	57.18 \pm 0.01	-0.04
+ FedIA	66.70 \pm 0.20	54.68 \pm 0.45	58.53 \pm 0.08	63.26 \pm 0.21	57.25 \pm 0.07	66.08 \pm 0.17	61.08 \pm 0.03	+3.86 $\uparrow^{3.90}$
FedProto	66.51 \pm 0.00	38.35 \pm 0.03	58.80 \pm 0.01	68.67 \pm 0.03	49.35 \pm 0.03	61.57 \pm 0.00	57.21 \pm 0.00	-0.01
+ FedIA	68.19 \pm 0.07	48.03 \pm 0.13	59.46 \pm 0.08	68.87 \pm 0.08	55.28 \pm 0.09	67.82 \pm 0.15	61.27 \pm 0.02	+4.05 $\uparrow^{4.06}$
FGSSL	67.40 \pm 0.05	38.84 \pm 0.03	59.04 \pm 0.02	69.01 \pm 0.04	49.63 \pm 0.03	62.17 \pm 0.10	57.68 \pm 0.02	+0.48
+ FedIA	68.27 \pm 0.04	48.64 \pm 0.02	60.29 \pm 0.03	69.41 \pm 0.05	54.03 \pm 0.04	68.00 \pm 0.09	61.44 \pm 0.03	+4.22 $\uparrow^{3.76}$
FGGP	67.98 \pm 1.35	65.72 \pm 0.37	56.85 \pm 0.91	66.18 \pm 1.35	56.12 \pm 0.71	69.07 \pm 0.41	63.65 \pm 0.42	+6.43
+ FedIA	72.27 \pm 0.50	49.72 \pm 2.04	62.05 \pm 0.39	75.03 \pm 1.07	54.99 \pm 5.20	68.92 \pm 0.84	63.83 \pm 1.19	+6.61 $\uparrow^{6.18}$

Table 5: Accuracy comparison on the **Twitch Gamers** domain skew setting (Robust-verify Setting; Ratio 1:5:1:1:1:1, 20 Clients). Results are reported as mean \pm std over the last 20 rounds. Methods are grouped pairwise (baseline vs. enhanced) with alternating gray shading. **Annotations:** The column Δ denotes the accuracy gap relative to generic FedAvg. The colored superscripts (e.g., $\uparrow^{4.80}$) indicate the specific performance gain achieved by FedIA compared to the **original baseline** in that group.

Methods	Domains						Overall	
	ES	DE	FR	RU	EN	PT	AVG	Δ
FedAvg	67.14 \pm 0.05	38.70 \pm 0.01	58.76 \pm 0.00	65.95 \pm 0.03	49.05 \pm 0.03	59.48 \pm 0.00	56.51 \pm 0.01	-
+ FedIA	67.80 \pm 0.09	55.51 \pm 0.05	59.61 \pm 0.02	64.31 \pm 0.05	57.45 \pm 0.02	59.61 \pm 0.02	61.31 \pm 0.02	+4.80 $\uparrow^{4.80}$
FedProx	66.61 \pm 0.00	38.39 \pm 0.00	58.64 \pm 0.00	66.07 \pm 0.02	59.08 \pm 0.00	59.08 \pm 0.00	56.13 \pm 0.00	-0.38
+ FedIA	70.44 \pm 0.18	54.41 \pm 0.08	59.06 \pm 0.10	68.13 \pm 0.08	57.71 \pm 0.06	59.06 \pm 0.10	62.96 \pm 0.03	+6.45 $\uparrow^{6.83}$
MOON	67.03 \pm 0.03	38.77 \pm 0.01	58.97 \pm 0.02	66.07 \pm 0.02	48.72 \pm 0.03	59.35 \pm 0.03	56.49 \pm 0.01	-0.02
+ FedIA	71.11 \pm 0.07	41.15 \pm 0.03	63.33 \pm 0.03	70.05 \pm 0.04	50.16 \pm 0.06	63.33 \pm 0.03	60.04 \pm 0.02	+3.53 $\uparrow^{3.55}$
FedDyn	50.00 \pm 21.94	50.00 \pm 11.05	50.00 \pm 14.02	50.06 \pm 24.00	50.00 \pm 4.47	50.00 \pm 14.31	50.01 \pm 9.79	-6.50
+ FedIA	68.16 \pm 0.57	55.14 \pm 0.44	58.13 \pm 0.85	66.74 \pm 0.48	56.25 \pm 0.90	58.13 \pm 0.85	61.42 \pm 0.31	+4.91 $\uparrow^{11.41}$
FedProc	67.04 \pm 0.03	38.72 \pm 0.02	58.77 \pm 0.03	65.94 \pm 0.03	48.88 \pm 0.02	59.41 \pm 0.07	56.46 \pm 0.01	-0.05
+ FedIA	64.36 \pm 0.04	60.05 \pm 0.02	55.28 \pm 0.03	62.09 \pm 0.08	57.64 \pm 0.02	67.99 \pm 0.04	61.23 \pm 0.01	+4.72 $\uparrow^{4.77}$
FedProto	67.15 \pm 0.02	38.66 \pm 0.02	58.71 \pm 0.02	65.96 \pm 0.00	48.98 \pm 0.02	59.46 \pm 0.04	56.48 \pm 0.01	-0.03
+ FedIA	74.06 \pm 0.00	38.95 \pm 0.00	64.02 \pm 0.00	71.94 \pm 0.00	45.53 \pm 0.00	64.02 \pm 0.00	59.80 \pm 0.00	+3.29 $\uparrow^{3.32}$
FGSSL	67.71 \pm 0.04	39.20 \pm 0.03	58.91 \pm 0.04	65.73 \pm 0.09	49.50 \pm 0.04	59.83 \pm 0.07	56.81 \pm 0.02	+0.30
+ FedIA	64.36 \pm 0.21	56.01 \pm 0.13	56.93 \pm 0.04	63.91 \pm 0.11	56.91 \pm 0.21	56.93 \pm 0.04	59.82 \pm 0.05	+3.31 $\uparrow^{3.01}$
FGGP	65.99 \pm 2.35	66.28 \pm 0.76	55.41 \pm 1.95	63.97 \pm 3.10	55.70 \pm 1.58	67.89 \pm 2.34	62.54 \pm 1.24	+6.03
+ FedIA	68.86 \pm 1.28	69.69 \pm 2.52	51.22 \pm 1.77	62.78 \pm 2.04	60.01 \pm 1.58	72.50 \pm 0.58	64.17 \pm 0.30	+7.66 $\uparrow^{1.63}$

guide local training, narrowing performance gaps on highly non-IID data. **FedProto** [Tan *et al.*, 2022] replaces gradient exchange with communication of class prototypes, which the server aggregates and redistributes to regularize heterogeneous client models. **FGSSL** [Huang *et al.*, 2024] tackles federated graph learning by jointly aligning node semantics and graph structures through self-supervised global-local contrast, enabling label-efficient training. **FGGP** [Wan *et al.*, 2024] learns domain-generalizable prototypes that decouple global and local representations, boosting cross-domain

transferability in federated graph settings. It is important to note that we did not include **FedSSP** as baselines in extensive experiments due to FedSSP [Tan *et al.*, 2024] follows the GSP methodology. Considering FedSage is an important baseline, we compare the performance with FedSage on GraphSage. This decision was made to maintain fairness in our comparisons.

Table 6: Ablation test on cross-domain setting by $mean_{\pm std}$ (%) calculated from last 20 rounds of totally 200 communication rounds. Δ calculates the AVG’s (average mean accuracy) difference in accuracy relative to FedAvg, while $AVG\Delta$ measures the average improvement of baselines which obtained with FedIA. All data is accurate to two decimal places.

FGL Methods	Different Domains of Twitch Gamers (Cross-domain Settings)						AVG	Δ
	ES	DE	FR	RU	EN	PT		
Setting 1	Domain Difference Ratio = 1:1:1:1:1:1 (12-Clients)							
FedAvg	66.46 \pm 0.02	38.38 \pm 0.02	58.84 \pm 0.03	68.74 \pm 0.03	49.36 \pm 0.02	61.57 \pm 0.00	57.22 \pm 0.01	–
FedAvg+FedIA-p	71.29 \pm 0.00	38.95 \pm 0.02	64.02 \pm 0.00	76.23 \pm 0.05	45.54 \pm 0.02	62.76 \pm 0.09	59.80 \pm 0.01	+1.78
FedAvg+FedIA	64.77 \pm 0.05	55.90 \pm 0.03	58.72 \pm 0.03	65.41 \pm 0.06	58.66 \pm 0.04	60.85 \pm 0.04	60.72 \pm 0.02	+3.50
Setting 3	Domain Difference Ratio = 1:10:1:1:1:1 (30-Clients)							
FedAvg	66.98 \pm 0.06	38.76 \pm 0.01	59.38 \pm 0.05	65.06 \pm 0.02	48.87 \pm 0.03	59.97 \pm 0.10	56.50 \pm 0.04	–
FedAvg+FedIA-p	<i>NA</i>	<i>NA</i>	<i>NA</i>	<i>NA</i>	<i>NA</i>	<i>NA</i>	<i>NA</i>	<i>NA</i>
FedAvg+FedIA	71.29 \pm 0.00	38.95 \pm 0.00	62.75 \pm 0.00	76.40 \pm 0.00	45.53 \pm 0.00	64.02 \pm 0.00	59.82 \pm 0.00	+3.32

Hyper-parameters

The hyperparameters of the FedIA framework include the mask ratio ρ and the momentum factor β . We defined the parameter search space for these hyperparameters as $\{0.1, 0.3, 0.5, 0.7, 0.9\}$. Due to space constraints, a detailed comparison and analysis of the hyper-parameters sensitivity can be found in next section.

A.2 Detailed Performance Analysis

In this section, we conduct a granular analysis of FedIA’s performance across a variety of challenging scenarios to verify its effectiveness and robustness.

Twitch Performance Analysis

To evaluate the robustness of FedIA under diverse organizational structures, we conduct experiments on the Twitch Gamers dataset across two distinct regimes: the balanced *Cross-domain* setting (Table 4) and the imbalanced *Domain-skew* setting (Table 5).

Performance under Balanced Cross-domain Shifts (Table 4). In this scenario (12 clients, Ratio 1:1:1:1:1:1), where data is evenly distributed across six regions, FedIA demonstrates exceptional compatibility with both general and specialized federated learning methods. As shown in Table 4, our framework achieves an average performance boost of **+4.71%** across all tested baselines.

- **Enhancing Traditional FL:** General optimizers such as FedProx and FedDyn, which are designed for statistical non-IID data, see significant gains of **+5.73%** and **+5.98%** respectively. This highlights that FedIA successfully resolves the structural mismatches that standard regularization-based methods fail to address.
- **Empowering Specialized FGL:** FedIA also proves complementary to existing FGL solutions. For instance, it further improves the state-of-the-art FGGP by **+6.61%** and FedProc by **+3.86%**, achieving the highest overall accuracy of **63.83%**.

Resilience under Severe Domain Skew (Table 5). Table 5 presents a more challenging “Robust-verify” setting (20 clients, Ratio 1:5:1:1:1:1), where the German (DE) domain dominates the network. FedIA remains the top performer across all baseline groups:

- **Rescue of Collapsed Strategies:** A notable result is observed for FedDyn. While the vanilla FedDyn baseline collapses under severe skew (dropping to 50.01% accuracy), the integration of FedIA restores its stability and boosts performance by **+4.91%**.
- **Robustness Across Baselines:** FedIA consistently elevates the performance of diverse architectures, including MOON (**+3.53%**), FedProc (**+4.72%**), and FedProto (**+3.29%**).
- **SOTA Peak Performance:** The combination of FGGP and FedIA reaches the peak accuracy of **64.17%**, representing a substantial **+7.66%** improvement over the standalone FGGP baseline.

Summary. The results across Tables 4 and 5 confirm that FedIA’s two-stage server-side calibration—Global Importance Masking and Confidence-Aware Momentum—is universally effective. By mitigating the “Consensus Collapse” caused by structural orthogonality, FedIA enables both generic and graph-specific FL methods to achieve superior generalization even under extreme domain shifts.

Ablation Test

To evaluate the individual contributions of FedIA’s two-stage framework, we conduct an ablation study using FedAvg as the basal optimizer. As shown in Table 6, we compare the standard FedAvg against two variants: (i) **FedAvg+FedIA-p**, which exclusively employs Stage 1 (*Global Importance Masking*), and (ii) the full **FedAvg+FedIA** framework. We select FedAvg for this study to ensure a clean analysis, as methods like FGGP introduce auxiliary prototype communication that would confound the direct assessment of our aggregation components.

Stage 1: Primary Engine for Denoising. The results in the balanced cross-domain setting (Setting 1) demonstrate that *Global Importance Masking* (Stage 1) is the primary driver of performance recovery. By identifying and preserving a subset of salient gradient coordinates, FedAvg+FedIA-p boosts the average accuracy from **57.22%** to **59.80%** ($\Delta = +1.78\%$). This confirms our hypothesis that filtering domain-specific structural noise is highly effective in mitigating the *Consensus Collapse* observed in earlier rounds. Stage 1 allows the model to lock onto shared structural patterns, pre-

venting sparse informative signals from being washed out by majority near-zeros.

Stage 2: Essential Stabilizer under Extreme Skew. The critical role of Stage 2, *Confidence-Aware Momentum Weighting*, becomes evident in the severe domain-skew scenario (Setting 3). In this challenging environment, the Stage 1-only variant (**FedAvg+FedIA-p**) fails to converge, resulting in **NA** (not available) values due to numerical instability. This failure suggests that under extreme skew, even an optimized mask cannot fully reconcile the high conflict between sparse updates, leading to gradient explosion or collapse. The full FedIA framework, however, remains robust, achieving **59.82%** accuracy ($\Delta = +3.32\%$). By dynamically down-weighting outlier updates through momentum-based reliability tracking, Stage 2 acts as an indispensable stabilizer that ensures safe optimization trajectories even when domains are highly orthogonal.

Synergistic Contribution. In summary, the ablation study reveals a clear synergy between the two stages:

- **Stage 1** provides the "precision" by extracting the structural consensus from the disjoint gradient coordinates (*Structural Orthogonality*).
- **Stage 2** provides the "robustness" by smoothing out the volatile update strengths inherent in cross-silo shifts.

Together, they form a complete solution that is both effective in standard scenarios and indispensable in extreme conditions

Hyper-parameter Robustness

Evaluating Robustness for a Plug-and-Play Method. The practical utility of a plug-and-play method like FedIA hinges on its robustness to hyper-parameter selection. An overly sensitive method would require costly, per-case tuning, undermining its ease of deployment. We therefore analyze the sensitivity of FedIA's two key hyper-parameters—the gradient mask ratio ρ and the influence-regularized momentum factor β —from two perspectives: the performance with optimal settings, as shown in Table 7, and the performance across a wide search space, visualized in Figure 9.

Low Sensitivity Across a Wide Hyper-parameter Space.

Figure 9 provides compelling visual evidence of FedIA's robustness. The heatmaps illustrate the average performance improvement over baselines across a grid of (ρ, β) values, for both the cross-domain (Setting 1) and severe domain-skew (Setting 3) scenarios. The large red-boxed areas indicate the wide range of hyper-parameter combinations that yield performance superior to the average of the unassisted baselines. This demonstrates that the significant performance gains reported in Tables 1, 2, and 3 are not contingent on finding a single, narrow "sweet spot." Instead, FedIA is effective across a broad spectrum of settings, which confirms its low sensitivity and reinforces its status as a true plug-and-play solution.

Optimal Settings and Confirmation of Core Insight.

While Table 7 lists the optimal (ρ, β) pairs for each specific baseline and setting, the key takeaway is that these optimal values often align with our core theoretical insights. Notably, a small mask ratio $\rho = 0.1$ frequently appears as the optimal choice across various scenarios, such as for FedAvg+FedIA in Setting 1 and for FedDyn+FedIA and FedProto+FedIA in

Table 7: The best hyper-parameter configurations for FedIA under various settings on Twitch.

Basal Methods	Setting1		Setting2		Setting3	
	ρ	β	ρ	β	ρ	β
FedAvg+FedIA	0.1	0.1	0.1	0.3	0.3	0.3
FedProx+FedIA	0.9	0.3	0.7	0.5	0.5	0.7
Moon+FedIA	0.3	0.1	0.1	0.9	0.1	0.9
FedDyn+FedIA	0.3	0.9	0.5	0.3	0.1	0.1
FedProto+FedIA	0.1	0.3	0.3	0.1	0.1	0.9
FGSSL+FedIA	0.1	0.1	0.1	0.1	0.1	0.3
FGGP+FedIA	0.3	0.5	0.5	0.3	0.3	0.9

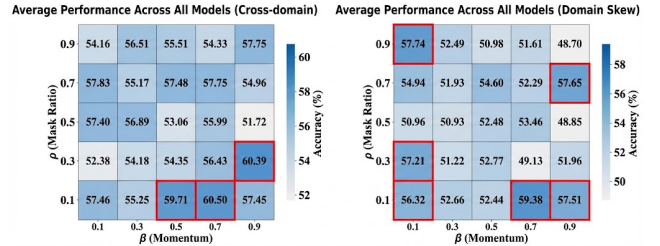


Figure 9: The effects of the hyperparameter variations are presented under setting 1 (cross-domain) and setting 3 (domain skew) on Twitch. The average performance of FedIA across six different methods has been calculated. The red box indicates the hyperparameter combinations that exceed the average value of the baseline without FedIA. This indicates that the superior performance of FedIA is not reliant on specific combinations of hyper-parameters but can be achieved through a wide range of general combinations.

Setting 3. This corresponds to a high pruning rate where only 10% of the most significant gradient coordinates are retained. This empirical result strongly supports our central hypothesis: a vast majority of gradient dimensions are dominated by domain-specific noise, and aggressively filtering these gradients is a highly effective strategy for robust federated graph learning. The observation that marginal values for ρ (e.g., 0.1) are often effective also provides a practical heuristic for efficient hyper-parameter search.

Conclusion on Robustness. In conclusion, the hyper-parameter analysis confirms that FedIA is not only effective but also robust. Its low sensitivity to the specific choices of ρ and β ensures that it can be deployed with minimal tuning to achieve reliable performance gains. This robustness, combined with the fact that its optimal performance aligns with the core "projection-first" principle of high-sparsity pruning, solidifies its standing as a practical and theoretically grounded solution for domain-robust federated graph learning.